Key material properties in crease cracking of kraft paper

BABAK MIRZAEI, TREY HARKSEN, SWAN SMITH, AND JOEL PANEK

ABSTRACT: Crease cracking of paperboard is important to control for the appearance and structural integrity of packages. Crease cracking is affected by creasing operation variables, as well as the physical properties of the paperboard. However, the effects of the physical properties are not clearly known.

The objectives of this work were to identify the key material properties that affect crease cracking and to clarify the effects of fiber composition and starch. Laboratory sheets were produced from bleached and refined softwood and hardwood commercial pulp at grammage and thicknesses that match a typical paperboard. To mimic papermaking operations, surface starch was applied via a bench-top size press. The sheets were creased in the lab over a range of penetration depths, and reverse-side cracking was measured. The results showed that less reverse-side cracking was correlated with higher tensile post-peak energy, a lower bending stress, and a lower z-direction (ZD) stiffness. The tensile post-peak energy is a measure of the resistance to crack growth via fiber-bridging. The bending force and the ZD stiffness influence the forces that create cracks. It was observed that decreasing the ratio of hardwood-to-softwood content and reducing the amount of starch would both decrease crease cracking.

Application: Key material properties that are identified in this study can be used to predict and minimize the crease cracking propensity of base paper. The effects of fiber composition and starch presence were studied for further insight.

Minimizing crease cracking of paperboard is important for packaging from visual and structural standpoints. Crease cracking is affected by the creasing operation variables, as well as the physical properties of paperboard. Recent work has identified methods for quantifying the creasing severity that drives cracking on the channel (bead) side [1]. However, the effects of the physical properties and structure on crease cracking are not clearly known to date. The central objective of this work is identifying the key material properties and their relationships that affect crease cracking on the channel (bead) side of the crease.

A number of papers have been published on cracking due to folding *without creasing*, including those on linerboard [2], coated paper [3-5], and coated laboratory sheets [6]. Cracking studies *with creasing* have included coated paper [1,7] and aluminum foil coated paper [8]. The general conclusion is that factors that increase the strain (or stress) on the surface due to bending will increase cracking, while factors that increase crack resistance (typically represented by strain at break or peak strength) will minimize cracking. The adhesion of coating to the substrate may also play a role. While this qualitatively makes sense and changes in materials and structure have been shown to influence the degree of cracking, a model that relates degree of cracking with properties and structure has not been validated for paperboard.

Cavlin introduced an empirical model for predicting the cracking of paperboard based on an energy balance and a brittleness parameter [9]. While the original equation was not supported with data, a variation of the equation did show a good correlation with cracking of corrugated board [10].

Finite element models of laminate structures have been developed that include elastic and plastic deformation and a "multi-linear failure criteria" [4] or maximum stress or strain criteria [11]. Varney and Bousfield developed a discrete element model for a coating layer only, based on three-point bending equations and a strain-to-failure criteria [12].

These studies highlight that there are several physical mechanisms involved in the creasing and folding sequence that can affect cracking. Both creasing and folding cause tension on the outer surface and cause shear and compression through the thickness [13]. The forces developed during creasing are a complex function of creasing conditions and material properties. The forces developed during folding are in principle more straightforward; complicated, however, by the state of the material after creasing, large deformations, and nonlinear response. Resistance to in-plane crack initiation and propagation can be quantified in multiple ways, including standard tensile properties, post-peak tensile properties, and fracture resistance parameters. However, the best method for this case is not obvious, because the cracks are likely initiated during the creasing process and then propagated during the folding process; the damage is localized on the surfaces, rather than bulk; and the stress zone is on the scale of millimeters. This is further complicated because the material is not homogenous or even a clearly defined laminate structure; commercial paperboard is an engineered structure of fibers, chemical additives, and coating.

Considering all of this, we decided to use an empirical approach, with the goal of minimizing the number of parameters and the complexity of the calculation. Experimentally, we evaluated uncoated laboratory sheets. The use of lab sheets allowed controlled investigation of simpler structures, which becomes a foundation for more complex structures. In our experiments, we chose to vary factors that we believed influenced cracking, including fiber type and surface starch. We used a systematic approach for quantifying cracking that was transferable across differences in thickness. The value of our approach is that this will help simplify the identification of key properties with their relative effect on cracking. The methodology can then be used as a foundation for more fundamental and rigorous models.

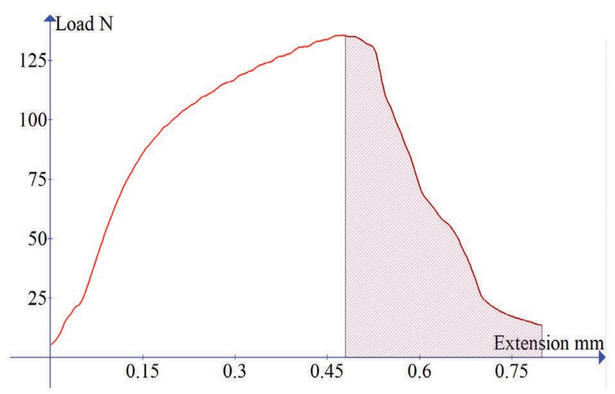

1. Typical load-deflection result from the short-span tensile test of a laboratory sheet. Highlighted area was used as an indication of fiber-bridging energy.

THEORY

Our belief is that failure is driven by stress, and the challenge is to determine the best criteria to describe the resistance to cracking, while developing a reasonable estimate of the stresses.

As a starting point, we consider the model introduced by Cavlin [9] to calculate a cracked length relative to the total creased length. The model is based on an energy balance and proposes that the relative crack length is proportional to the ratio of short-span compression strength (σ_C) to tensile strength (σ_T) divided by modulus of brittleness (L_c) and multiplied by an effective tensile span (L) (Eq. 1). Essentially, the cracking resistance is described by the post-peak fracture energy, while the driving force is described by the compression strength, as shown in an alternate derivation of the equation (Eq. 2):

$$\frac{l}{l_0} = \frac{L}{L_c}\left(\frac{\sigma_c}{\sigma_T}\right)^2 \quad (1)$$

$$\frac{l}{l_0} = \frac{L}{2 \cdot E \cdot J_{postpeak}}(\sigma_c)^2 \quad (2)$$

$$L_c = \frac{2 \cdot E \cdot J_{postpeak}}{{\sigma_T}^2} \quad (3)$$

The modulus of brittleness is defined as the post-peak fracture energy in tension divided by the pre-peak energy, which is claimed to indicate a critical material length for complete fracture. The ratio of compressive to tensile strength is assumed to be an indicator of the stress state of the convex surface at fold. The effective tensile span is defined by the system.

We propose that the driving force can be more effectively described by using a direct measure of bending stress and including the z-direction (out of plane) compressive modulus. The board is under bending and ZD compression during both creasing and folding and including both is expected to give a more robust characterization than any single parameter. In this case, the bending stress is defined as the initial peak moment for a 10-mm bending length, since this gives the maximum value on a similar size scale as creasing and folding. Bending stiffness has been suggested to be inversely related to fold-crack resistance [4] and was utilized to predict the onset of paper cracking at fold. However, bending stiffness cannot be used to indicate the cracking degree that occurs well beyond the elastic limit. Failure stress in bending is a more relevant property in this case. It is also important to note that bending stress relates to the development of a non-uniform stress field.

Post-peak energy, which was included in Cavlin's model, is an indicator of resistance to cracking. We believe cracking is a fracture process and therefore could be related to fracture toughness. There are a few methods developed for paper materials based on a fracture energy approach. We determined post-peak energy from a short-span tension test method developed by Tryding [14]. **Figure 1** displays an example of a load-deflection curve from a short-span tensile test, with the post-peak energy highlighted. Using a short gage length (5 mm), it is possible to capture the post-peak load vs. displacement curve, since the elastic energy stored in the short test strip is less than the amount of energy required to propagate any damage. Furthermore, size scale is known to affect the measurement of tensile properties [15], and the shorter span length will likely represent the local deformation due to creasing. We discuss these assumptions further in the next section.

The *stability index* introduced here utilizes three parameters: ZD modulus and bending stress as crack driving force with a negative effect on stability; and post-peak energy as

Sample Code	Thickness of Creased Sheets, mm	Specific ZD Modulus, kNm/kg	Specific Bending Strength, kNm/kg	Specific Tensile Post-Peak Energy, Nm^2/kg	Specific Short-Span Tensile Strength, kNm/kg	Specific Short-Span Compression Strength, kNm/kg
Unsized-20-1	0.31 (0.025)	217 (33)	41 (3.2)	5 (0.7)	46 (2.6)	23 (2.1)
Unsized-50-1	0.299 (0.025)	280 (22)	42 (3.5)	8 (1.4)	54 (4.6)	24 (1.9)
Unsized-80-1	0.302 (0.009)	236 (34)	48 (2.6)	12 (1.7)	62 (4.8)	25 (1.9)
Unsized-20-2	0.303 (0.022)	202 (4)	41 (2.1)	7 (0.9)	51 (3.3)	21 (1.4)
Unsized-50-2	0.28 (0.009)	225 (42)	41 (1.9)	11 (1.5)	55 (4.1)	23 (1.3)
Unsized-80-2	0.263 (0.004)	266 (17)	42 (2.7)	17 (2.4)	64 (5.6)	24 (1.6)
Sized-20-1	0.288 (0.006)	376 (48)	47 (2.6)	9 (1)	68 (4.7)	28 (1.4)
Sized-50-1	0.307 (0.003)	358 (55)	49 (3.6)	10 (1.5)	70 (6.8)	29 (1.8)
Sized-80-1	0.305 (0.02)	428 (72)	50 (3.4)	13 (2.1)	75 (5.6)	31 (2.8)
Sized-20-2	0.332 (0.021)	407 (11)	45 (2.4)	10 (2.4)	56 (3.5)	26 (1.3)
Sized-50-2	0.282 (0.024)	450 (59)	47 (3.4)	13 (3.1)	59 (4.8)	26 (0.7)
Sized-80-2	0.335 (0.013)	458 (56)	52 (3.1)	15 (2.7)	60 (6.1)	27 (1.5)

I. Physical properties of the laboratory sheets. Numbers in brackets are 1 standard deviation of the measurements. Sample code represents softwood percent followed by experiment number (ZD = z direction).

resistance to cracking with a positive effect on stability. In summary:

$$Stability\ index = \frac{resistance}{driving\ force} = \frac{J_{postpeak}}{\sigma_b\ E_{ZDC}} \quad (4)$$

$$\sigma_b = \frac{6M}{bt^2} \quad (5)$$

$$Cracking\ severity \propto \frac{1}{Stability\ index} \quad (6)$$

where $J_{postpeak}$ is post-peak energy from tensile load-deflection curve per fractured sectional area, and σ_b is maximum bending stress up to 30° of rotation at 10 mm bending length. M, b, and t are moment, sample width, and thickness, respectively. The $6/(bt^2)$ is obtained from the ratio of area moment of inertia-to-distance of neutral plane from surface. E_{ZDC} is ZD compressive modulus.

Since the caliper and basis weight of the sheets made in the lab typically vary, we normalized all properties presented in this article, except bending stress, by basis weight of the individual sheets used per test. The σ_b was normalized by sheet density, as thickness was needed in the equation. **Table I** presents several physical properties of the studied samples.

METHODS AND MATERIALS

Lab sheet production

Handsheets (305 mm x 305 mm) with a target basis weight of 190 g/m^2 were made using bleached softwood and hardwood pulp produced in a commercial paper mill. The pulp was collected after the stock preparation refiners and did not have any chemical additives.

Hardwood and softwood pulps were combined to target 20%, 50%, and 80% softwood content. Using the consistency of the pulp as determined by TAPPI Standard Test Method T 240 “Consistency (concentration) of pulp suspensions,” the size of the sheet, the target mass, and the required wet mass of the pulp was calculated. The appropriate amounts of softwood and hardwood pulps were weighed, combined, and mixed.

For handsheet production, TAPPI T 205 “Forming handsheets for physical tests of pulp” was used with the following modifications: 305 mm x 305 mm (12 in. x 12 in.) sheet machine (G-100, Adirondack Machine Corp; Hudson Falls, NY, USA) with appropriately sized components; target basis weight of 190 g/m^2; and pressing and drying as given in the following description.

The wet handsheets were pressed in a hydraulic press as a stack of sheets and blotter papers sandwiched between metal plates. Two pressing cycles were done at 345 kPa (50

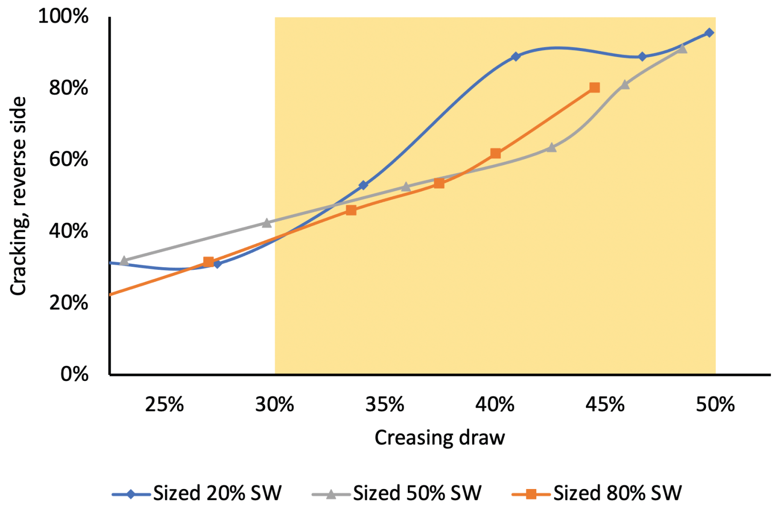

2. Typical cracking charts used in this study. Each point represents the average of three measurements. All cracking results were averaged over the highlighted 30%–50% creasing draw range (SW = softwood).

psi) for 2 min each, with the wet blotters replaced with dry blotters in between the cycles. The settings were selected to achieve the target caliper. The pressed sheets were then dried under restraint in TAPPI conditions (50% relative humidity [RH], 23°C) for at least 24 h. The sheets were restrained by keeping them attached to the metal plates, placing rubber stoppers along the edges of the sheets, and building a stack of plates and rubber stoppers, with a weighted plate on top.

Surface starch was applied to half of the sheets for each pulp blend set. A bench-top size press (Werner Mathis AG; Oberhasli, Switzerland) was used in pond mode to apply starch to both surfaces. A total addition of 25 g/m^2 was targeted. The starch solution was prepared by cooking raw starch (Ethylex 2015, Tate & Lyle; London, UK) to 88°C (190°F) for 30 min at a solids content of 10%–13%. The size press nip pressure was set to 300 kPa (44 psi), and the speed setting was 4 m/min. Starch solution was added to flood the closed nip, and then the handsheet was passed through the nip. The wet sheets were weighed to determine the amount of starch picked up. The starched sheets were placed on metal plates and dried under restraint in TAPPI conditions using the same technique as for the pressed sheets.

Physical testing

Samples were conditioned and tested at TAPPI conditions (50% RH, 23°C). Basis weight and caliper were measured on each of the handsheets. The following physical tests were performed with at least six replicates per condition: short-span tensile test (Instron universal testing machine 5965); bending test (L&W bending tester code 160, Lorentzen & Wettre; Stockholm, Sweden) according to TAPPI Standard Test Method T 556 “Bending test of paper and paperboard by single-point bending method”; and ultrasonic ZD modulus (OPUS 3-D, Sonisys; Atlanta, GA, USA). A custom clamp was used for the short-span tensile tests, described in [16] and [17]. The tensile test span length was 5 mm and width was 15 mm; rate was 0.05 mm/s. Bending test was completed with a 38-mm wide test piece at a 10-mm bending length, with force measured up to 90° bending.

Creasing and cracking evaluation

The creasing procedure is described in [1,18]. Strips (102 mm x 305 mm) were cut from the handsheets. Before lab creasing, the paper strip was printed with a water-based black ink (Flint Box II black, Flint Group; Luxembourg) using an ink proofer (Harper Scientific Phantom Proofer, Harper Corp. of America; Charlotte, NC, USA) with a 12.25 BCM anilox roll at a speed setting of 85-90. Printing was done to maximize contrast for visualizing cracks at the crease (note that the previously described method of using iodine staining [1] did not provide a consistent contrast for both the starched and non-starched samples). The strips were conditioned and creased at TAPPI conditions (50% RH, 23°C). Creasing was done with a rule width of 0.35 mm (flat tip), channel width of 1.00 mm, and penetration depths ranging from 0.05 to 0.25 mm, under a strip tension of 1 kN/m. The strips were oriented so that the printed surface was on the channel side (bead side of the crease), since the goal was to evaluate cracking on this side. After creasing, the strip was trimmed to 38-mm wide and folded to 180° away from the printed surface. Crack length was measured on the printed (channel/bead side) surface while folded to 180°. The cracking degree is expressed as a percent of the total length of the crease that shows cracks. The deformation of paper in the crease is expressed as the creasing draw, which takes into account the effects of crease depth, tool geometry, and paper thickness [1]. **Figure 2** shows

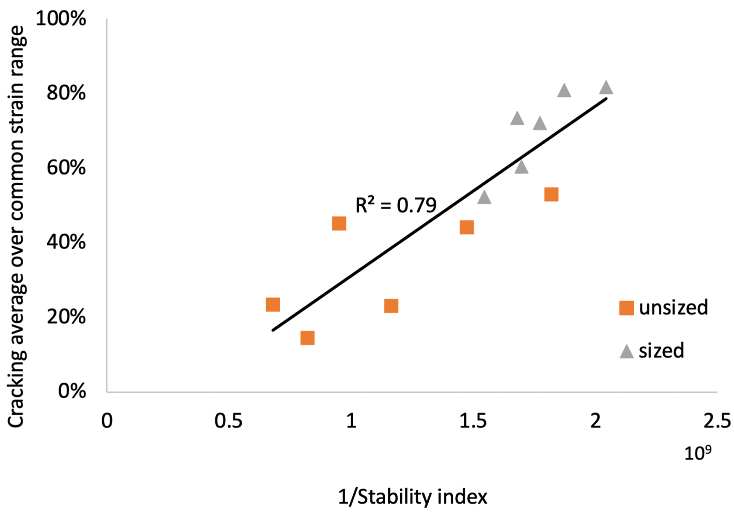

3. The effect of proposed physical properties on measured cracking.

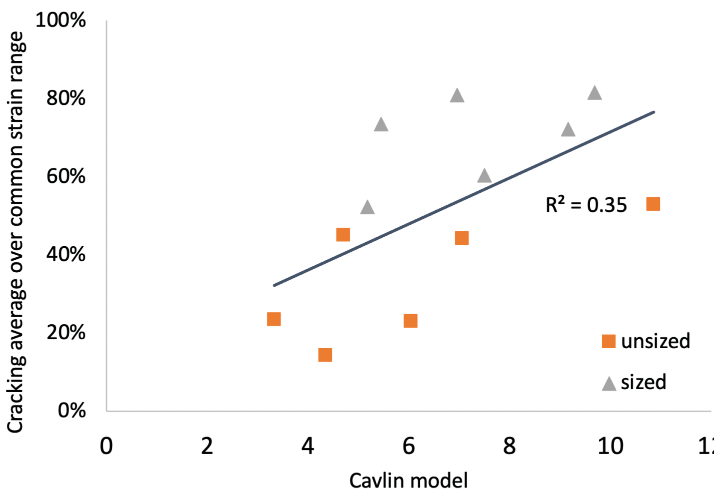

4. Cavlin model using crease strain.

typical results for the lab sheets studied here. Note that the critical draw concept described in [1] was not used here, because the cracking degree did not go below the 5% criteria for the majority of the samples, thus the critical draw could not be determined consistently. Instead, we selected a common creasing draw range (30%–50%) for all samples and then averaged the cracking degree over this range. This allows a comparison of the samples under the same range of creasing deformation. Therefore, geometric parameters—including the penetration depth of the rule and paper thickness—have been considered in creasing strain calculation at the previously mentioned range.

RESULTS AND DISCUSSION

This evaluation aimed to clarify the key properties that affect crease cracking and to establish their relative effect. It was built on the premise that crease cracking is a fracture process and key properties either drive cracking or resist it.

Figure 2 shows examples of cracking degree vs. creasing draws for three conditions. Cracking degree was averaged over the highlighted area (30% to 50% creasing draw) per condition. The average cracking degree across this range gives a robust representation of each condition, since a common deformation range is used; that is, the extremes are excluded and the differences in thickness are normalized by using the creasing draw.

Figure 3 shows a good correlation between the average cracking degree and the proposed stability index, demonstrating the validity of the selected properties. The subgroups are in line with each other and follow the same trend. While there is scatter in the data, it is clear that a sample with a high stability index (low inverse) will perform significantly better than one with a low stability index (high inverse). **Figure 4** shows that Cavlin's model trends

Model	Equation	Driving Force	Crack Resistance	Overall Adjusted R^2	Sized Subgroup R	Unsized Subgroup R
A	$E_{ZDC}*\sigma_b/J_{postpeak}$	$E_{ZDC}*\sigma_b$	$J_{postpeak}$	0.77	0.86	0.75
B	$EZDC*\sigma_b/\sigma T$	$EZDC*\sigma_b$	$J_{postpeak}$	0.42	-0.46	0.76
C	σ_b/Jpostpeak	σ_b	$J_{postpeak}$	0.06	0.77	0.63
D	σ_c/Jpostpeak	σ_c	$J_{postpeak}$	0.00	0.72	0.66
E Cavlin model	$(1/L_c)*(\sigma_c/\sigma_T)^2$ $=1/(2*E*J_{postpeak})*\ \sigma_c^2$	σ_c^2	$E*J_{postpeak}$	0.28	0.53	0.71

II. Correlation between various physical properties and measured cracking.

in the right direction, but shows more scatter. Although the application of this model was originally demonstrated for corrugated boards only, it is still directionally valid for our samples, and it is worth understanding what is causing the differences in the fit.

Table II includes additional parameters and combinations that have been evaluated and highlights that the model with post-peak energy, bending force, and ZD modulus gives the best fit. Comparison of models A and B demonstrate that post-peak energy is a better measure of cracking resistance than peak stress; post-peak energy better describes the progressive nature of crack formation. There is a progressive increase in damage and the size of the cracks due to an increase in creasing severity, not just a catastrophic failure. The structure maintains integrity due to fiber bridging, and there is limited energy to grow cracks due to the size scale.

Comparison of model A with C and D show that for the driving force, the combination of bending force and ZD modulus gives a better fit than either bending force or short-span compression force alone. While this combination introduces additional parameters, it is recognized that each can have an independent effect on the tensile force on the surface.

As discussed previously, the bending force gives a direct measure of the tensile force on the surface, while short-span compression gives an estimate. There is a reasonable correlation between compressive and bending stresses, as shown in **Fig. 5**, but there is enough scatter to question the accuracy of the short-span compression test as an estimator. It is important to note that for surface sized and/or coated boards, which exhibit significant ZD profile of properties, the bending test can reflect the area moment of inertia of the internal structure of the material while the in-plane compressive test does not have this ability.

It is logical that the ZD modulus can have an independent effect on the tensile force on the surface. It has been proposed that damage under bevel blade subjected to pushing load is proportional to the ZD compressive stiffness if other variables are kept constant [19,20]. This means a sheet

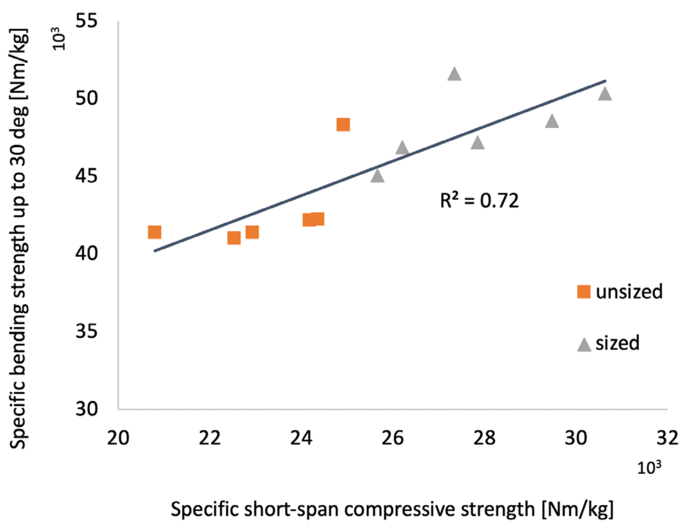

5. Correlation between compressive and bending strength.

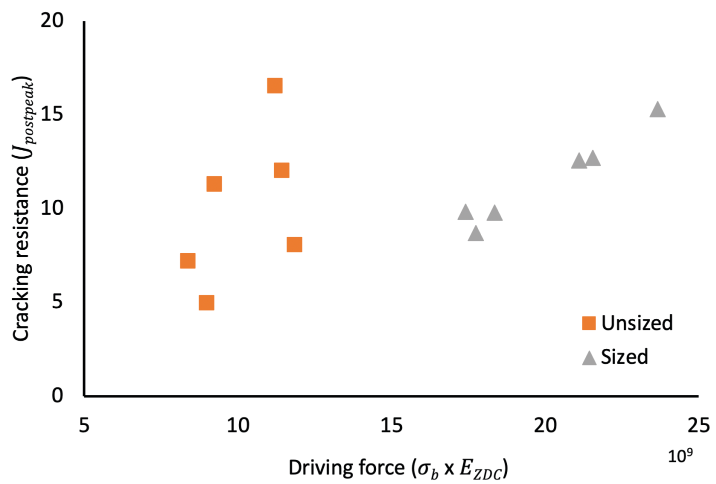

6. Materials selection chart to minimize crease cracking.

that is stiffer in ZD can be cut easier (i.e., more damage), which is the opposite of the creasing objective to avoid cracking. In our case, the paper is compressed by the rule during creasing, and a higher ZD modulus means that more stress is transferred to the surface opposite the creasing rule. It is therefore very likely that ZD stiffness contributes to the surface damage and cracking caused by creasing and subsequent folding. Since failure in ZD compression is hard to define, we instead utilized modulus measured consistently by an ultrasound device.

The main differences with the Cavlin model are that it includes a *squared* term for compressive strength and does not include a ZD modulus, but does include an in-plane modulus. The model is thus more sensitive to the compressive strength, which has limitations as an accurate predictor. We demonstrated that including ZD modulus provides an improvement. The in-plane modulus does not appear to have an independent effect on cracking, so its inclusion in the model likely causes more scatter rather than more accuracy.

Describing the driving force with only the bending stress and ZD compression is simplistic, but effective. While the actual stress state during creasing and folding is complex, these two terms capture the essential differences in materials that influence cracking. Bending stiffness and cracking resistance have been suggested to be inversely related [4]. High bending stress implies that the compressive side is relatively strong, and more stress is concentrated on the tensile side. The ZD compression is important, because the dynamic creaser rule impacts the board in ZD in the creasing operation to cause the delamination needed for folding. Boards that deform easier under compressive load (less stiff) develop less stress and are likely to crack less.

The three parameters identified here can thus efficiently estimate differences in the cracking degree due to the material properties and can then be used to better understand what is causing differences in performance and what can be done to improve performance. Because many properties are interrelated in papermaking, this gives better guidance on how process parameters should be optimized.

Figure 6 separates the stability index into the cracking resistance (crack propagation energy) and crack driving force (ZD modulus x bending stress) components. This can be used as a selection/optimization guide. The cracking is minimized when the ratio of cracking resistance to crack driving force (stability index) is maximized. Therefore, using this selection criterion, a guideline on this chart with a relatively high slope can identify the sheets with better performance. The results displayed on this chart clearly separate sized and unsized sheets, indicating the adverse effect of surface starch on cracking. In this case, the cracking increases because the driving force increases, not because the cracking resistance decreased. Ideal cracking performance should be targeted on the upper left side of this chart.

The reciprocal of stability index with the corresponding measured cracking is shown in **Fig. 7**. This chart summarizes the effects of the studied variables as follows: softwood content improved the stability index and therefore would reduce cracking, while surface sizing adversely affected the stability index. The adverse effect of starch presence in pre-coating layer on fold cracking has been reported in the literature [5]. We applied starch symmetrically on the sheets for surface sizing. Overall, predicted and measured cracking follows a similar trend for both experiments. It is important to note that cracking is a scattered property in nature and even sophisticated models may not exhibit excellent predictability.

Youn et al. suggested that improvement to physical properties by either the addition of more softwood fiber or more pulp beating would adversely affect the cracking of coated lab sheets [6]. However, they did not crease before folding, they did not consider the role of out of plane physical properties, and their sheets were coated, which would imply the

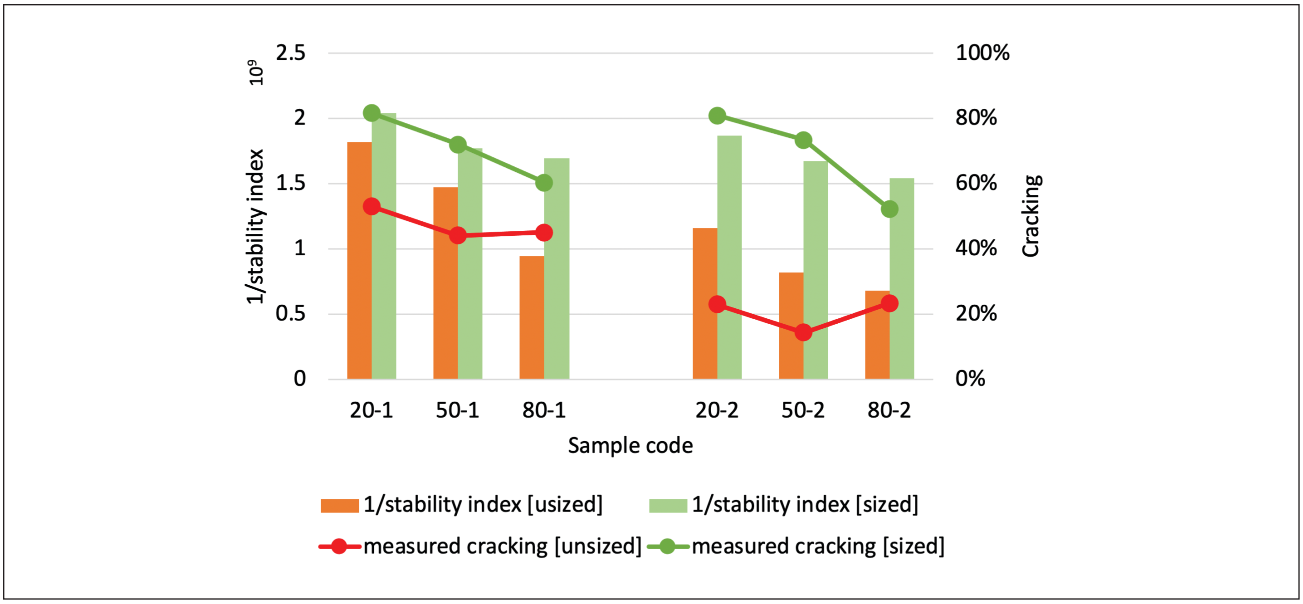

7. Comparison of cracking and proposed physical properties of sized and unsized sheets for various fiber compositions. Sample code represents softwood percent followed by experiment number.

importance of the balance between the coating and base paper properties. Based on our experiments, the conventional belief that the long, flexible softwood fibers can help reducing cracking is valid. Long fibers have been reported to be extremely beneficial for the fracture toughness of kraft paper [21]. The length weighted average fiber length was about 2.4 mm and 0.9 mm for our softwood and hardwood pulps, respectively.

CONCLUSIONS

Creasing and folding of paperboard is a complicated process that can cause cracking, and it indeed depends on many properties and variables. The simple model that identifies the critical properties that can be measured by a few lab tests provides a useful tool to evaluate cracking propensity. The model utilizes three physical properties, namely, ZD compressive modulus, bending stress, and post-peak fracture energy as shown in the equation below:

$$Stability\ index = \frac{resistance}{driving\ force} = \frac{J_{postpeak}}{\sigma_b\, E_{ZDC}}$$

The conclusions from this study are summarized as follows:

- Reverse-side cracking degree correlated well with the reciprocal of a stability index, defined as the post-peak energy divided by the product of bending stress and ZD modulus.
- The post-peak energy provided a relevant measure of cracking resistance, because the cracking represents progressive damage to the surface, not just a catastrophic failure.
- The bending stress and ZD modulus provided a measure of the driving force that causes cracking. While they do not give a rigorous calculation of stresses, they highlight the factors that cause differences.
- The use of the stability index with cracking resistance and driving force components allowed better interpretation on how process factors affect cracking. For instance, changes in starch amount influenced both the cracking resistance and the driving force; in this case, the increase in driving force was more detrimental than the increase in cracking resistance. However, increasing softwood to hardwood content improved the stability index and therefore reduced cracking. **TJ**

LITERATURE CITED

1. Panek, J.C., Smith, S.D., and Coffin, D.W., *TAPPI J.* 19(4): 219(2020).
2. Popil, R.E., "Prediction of fold-cracking propensity through physical testing," *TAPPI PaperCon*, TAPPI Press, Peachtree Corners, GA, USA, 2010.
3. Barbier, C., Larsson, P.-L., and Östlund, S., *Nord. Pulp Pap. Res. J.* 17(1): 34(2002). https://doi.org/10.3183/npprj-2002-17-01-p034-038.
4. Alam, P., Toivakka, M., Carlsson, R., et al., *J. Compos. Mater.* 43(11): 1265(2009). https://doi.org/10.1177/0021998308104227.
5. Oh, K., Sim, K., Jeong, Y.B., et al., *Nord. Pulp Pap. Res. J.* 30(2): 361(2015). https://doi.org/10.3183/npprj-2015-30-02-p361-368.
6. Youn, H.J., Sim, K., Oh, K.D., et al., *Nord. Pulp Pap. Res. J.* 27(2): 445(2012). https://doi.org/10.3183/npprj-2012-27-02-p445-450.
7. Rätto, P., Hornatowska, J., and Barbier, C., *Nord. Pulp Pap. Res. J.* 27(4): 714(2012). https://doi.org/10.3183/npprj-2012-27-04-p714-720.
8. Nagasawa, S., Endo, R., Fukuzawa, Y., et al., *J. Mater. Process. Technol.* 201(1-3): 401(2008). https://doi.org/10.1016/j.jmatprotec.2007.11.253.
9. Cavlin, S., *Packag. Technol. Sci.* 1(2): 77(1988). https://doi.org/10.1002/pts.2770010206.

10. Cavlin, S. and Edholm, B., *Packag. Technol. Sci.* 1(1): 25(1988). https://doi.org/10.1002/pts.2770010107.
11. Barbier, C., Larsson, P., and Östlund, S., *Compos. Struct.* 67(4): 383(2005). https://doi.org/10.1016/j.compstruct.2004.01.024.
12. Varney, D. and Bousfield, D., *TAPPI J.* 18(2): 101(2019). https://doi.org/10.32964/TJ18.2.101.
13. Coffin, D.W. and Nygårds, M., "Creasing and folding," in *Advances in Pulp and Paper Research, Oxford 2017, Trans. of the XVIth Fund. Res. Symp. Oxford, 2017* (W. Batchelor and D. Söderberg, Eds.), FRC, Manchester, 2018.
14. Tryding, J. and Gustafsson, P.-J., *TAPPI J.* 83(2): 84(2000).
15. Hagman, A. and Nygårds, M., *Nord. Pulp Pap. Res. J.* 27(2): 295(2012). https://doi.org/10.3183/npprj-2012-27-02-p295-304.
16. Tryding, J., Marin, G., Nygårds, M., et al., *Int. J. Damage Mech.* 26(6): 895(2017). https://doi.org/10.1177/1056789516630776.
17. Marin, G., Nygårds, M., and Östlund, S., "Stiffness and strength properties of five paperboards and their moisture dependency," *Int. Pap. Phys. Conf.*, TAPPI Press, Peachtree Corners, GA, 2019.
18. Coffin, D.W. and Panek, J.C., *TAPPI J.* 17(4): 231(2018). https://doi.org/10.32964/TJ17.04.231.
19. Chaijit, S., Yajima, Y., Kikuchi, K., et al., *Mater. Sci. Forum* 594: 39(2008). https://doi.org/10.4028/www.scientific.net/MSF.594.39.
20. Mitsomwang, P., Nagasawa, S., Chaijit, S., et al., *J. Adv. Mech. Des. Syst. Manuf.* 6(7): 1168(2012). https://doi.org/10.1299/jamdsm.6.1168.
21. Larsson, P.T., Lindström, T., Carlsson, L.A., et al., *J. Mater. Sci.* 53: 3006(2018). https://doi.org/10.1007/s10853-017-1683-4.

ABOUT THIS PAPER

Cite this article as:
Mirzaei, B., Harksen, T., Smith, S., et al., *TAPPI J.* 20(2): 81(2021). https://doi.org/10.32964/TJ20.2.81

DOI: https://doi.org/10.32964/TJ20.2.81

ISSN: 0734-1415

Publisher: TAPPI Press

About this journal

ABOUT THE AUTHORS


Mirzaei

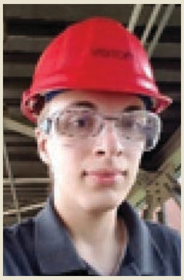
Harksen


Smith


Panek

Although this topic is quite important to the paper packaging industry for avoiding cracking in the converting process, the current knowledge addressing material properties that influence crease cracking is rather limited. Our work here significantly supplements the current knowledge on this matter.

We quantitatively compared results from this research to previous works aimed at addressing a similar objective. We also discussed various approaches from the literature and the present findings.

The most challenging aspect of this research was the analysis of crease cracking and other physical properties of the samples prepared at different conditions. Through this work, we found the considerable importance of non-traditional physical properties on converting performance. It was interesting to discover that crease cracking can be predicted by a few quick lab tests instead of tedious creasing and cracking evaluation.

Mills can use this information to identify physical properties that can be engineered to minimize crease cracking. Our next step is evaluation/establishment of other methods for fracture properties of paperboard that address crack propagation.

Mirzaei is senior R&D scientist; Harksen in former R&D intern; Smith is senior R&D researcher; and Panek is principal R&D scientist at WestRock, Richmond, VA, USA. Email Mirzaei at babak.mirzaei@westrock.com.